# ON THE SHIP MOTIONS IN SHALLOW WATER

Takaki, Mikio
Research Institute for Applied Mechanics, Kyushu University : Research Associate

https://doi.org/10.5109/6613538

出版情報：Reports of Research Institute for Applied Mechanics. 25 (80), pp.133-166, 1978-03.
九州大学応用力学研究所
バージョン：
権利関係：

Reports of Research Institute for Applied Mechanics
Vol. XXV, No. 80, 1978

# ON THE SHIP MOTIONS IN SHALLOW WATER*

By Mikio TAKAKI**

The auther has measured amplitudes of motions of a tanker ship model with various heading angles in regular waves at a shallow water tank. The experimental results are compared with ones of theoretical calculations obtained by the so-called "New Strip Method". It becomes clear from the above comparisons that the results of theoretical calculations according to new strip method agree approximately with the experimental results in oblique waves, and especially the theoretical values and experimental ones with zero-advancing speed agree very well in beam sea condition.

## 1. Introduction

Because of increasing dimensions of ships in recent years, several sea depths of her trade routs and her working area have been becoming relatively shallow. The reduction of sea depth may lead to hit or grand the bottom of sea. It therefore has been becoming a great important problem to predict ship motions and the hydrodynamic forces acting on ships in waters of finite depths, in which ships can operate safely. The studies of ship motions in water of finite depth, however, have been limited according to comparing with those in water of infinite depth. Now we can classify the theoretical studying methods of ship motions in waters of finite depths into three groups as follows.

(a) Method of strip theory.
(b) Method of slender body theory.
(c) Method of three dimensional calculation due to the distributions of sources.

Firstly as for (a) method by strip theory, C. H. Kim calculated the longitudinal motions of the tanker ship in head sea conditions[1] and at the same time estimated the bending moments of the midship section[2]. Hooft carried out various experiments by using the model ship of Series-60 with $C_B=0.8$ in a shallow water tank and obtained valuable data[3]. But he did not calculate the precise hydrodynamic forces in waters of finite depths and predicted approximately the longitudinal motions by revising the values of hydrodynamic forces on a ship in deep water.

* This paper is translated from Transactions of the West-Japan Society of Naval Architects, No. 54, 1977.
** Research Associate, Research Institute for Applied Mechanics, Kyushu University.

Secondly as for (b) method by slender body theory, Tuck obtained the equations of ship motions in all six degree of freedom at zero forward speed in shallow water.[4] Futhermore Beck & Tuck calculated the amplitudes of five modes of Series-60 ship model with $C_B=0.8$ except for rolling motion.[5] But they did not carry out the experiment to compare with their calculated values and it has not been become obvious that their method is useful enough for practical usage.

As for the third method (c) by three dimensional calculating method, Oortmerssen recently calculated the ship motions in all six freedom at no forward speed and the hydrodynamic forces and moments acting on a sihp body in water of finite depth and at the same time carried out the various kinds of experiments.[6] He said that ship motions were affected significantly due to three dimensional effects of water bottom in shallow water.

The methods of (b) and (c) are very complicated to calculate numerically motions of ships except for the method of (a). Especially the method of (c) is impossible to predict ship motions with a forward speed at present time and can not be used for studying of the sea-keeping qualities with a forward speed. On the other hand, as for the method of (a) which has been useful to predict the sea-keeping qualities in water of infinite depth, it has not become clear to be useful enough for practical usage in waters of finite depths because of very little experimental varifications. It is therefore desired that correlation works between theoretical and experimental investigation should be performed and extended to oblique waves on water depths smaller than twice draft of a ship.[7]

When the strip method is available for predicting motions of a ship in waters of finite depths, two dimensional hydrodynamic forces and moments acting on body of a ship are required according to the assumption of strip theory. In previous papers,[8,9] the author calculated precisely two-dimensional hydrodynamic forces and moments acting on a cylinder with an arbitrary cross section by using a close fit method in which singularities were distributed on a surface of a cylinder, and showed that these calculated results were in good agreement with the experimental results obtained by forced oscillating tests.

In this paper, the amplitudes of motions of a tanker ship model with various heading angles have been measured in regular waves at a shallow water tank. The experimental results are compared with the theoretically calculated ones obtained by the so-called "New Strip Method." The availability of strip theory estimating motions of a ship in waters of finite depths is discussed according to the above correlation works.

## 2. Calculations of ship motions

Since two-dimensional hydrodynamic forces and moments acting on a cylinder with an arbitrary cross section in waters of finite depths have been

precisely estimated in previous papers[8,9], we have calculated the radiation forces and the wave exciting forces acting on a tanker ship model in waters of finite depths where the ratios of water depth and draft are 2.1 and 1.5 and have finally estimated the response curves of motions in oblique waves. The ship model is the tanker ship designed by the Ship Research 154-Meeting and the principal dimensions of the ship model and the body plan are shown in Table 2.1 and Fig. 2.1 respectively. When a ship operates in shallow water, there happen to sinkage and trim of a ship and consequently the cross sectional forms under a surface of water change a little. But as for this calculating motions of the ship we negrect these displacements as small quantities and estimate the amplitudes of the ship motions.

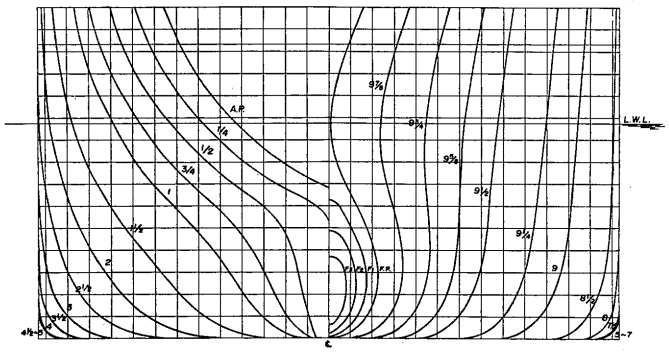


Fig. 2.1 Body plan of the ship model

Table 2.1 Principal dimensions of ship model

| | | |
|---|---|---|
| Length between perpendiculars | $Lpp$ | = 2.5 m |
| Breadth of ship | $B$ | = 0.5 m |
| Draft | $T$ | = 0.183 m |
| Displacement | $\Delta$ | = 187.58 Kg |
| Block coefficient | $C_B$ | = 0.82 |
| Metacentric height | $\overline{GM}$ | = 0.051 m |
| Height of gravity from water line | $\overline{\text{XX}G}$ | = 0.023 m |
| Distance of gravity from midship | $\overline{OG}$ | = 0.077 m |
| Radius of longitudinal gyration | $K_l$ | = 0.239 $Lpp$ |
| Radius of transverse gyration | $K_t$ | = 0.332 $B$ |
| With bildge-keel | $b_{B\cdot K\cdot}$ | = 10 mm |
| | $l_{B\cdot K\cdot}$ | = 0.25 $Lpp$ |
| With propeller and rudder | | |

## 2.1 Equations of ship motions in oblique waves

As shown in Fig. 2.2, $O'$-$X_1Y_1Z_1$ is a cordinate system fixed in space, in which a regular waves $\zeta_a$ progresses to the direction $X_1O'$ and a ship is navigating in the direction $O'X$ at an angle $\chi$ to the direction $O'X_1$. Let $O'$-$XYZ$ be a new coordinate system fixed in space, and let $o$-$x_by_bz_b$ be a coordinate system fixed in ship body, where $o$ is the intersection of the centerline of the ship and the midship in a surface of water. And let $o_0$-$xyz$ be a coordinate system which is moving with a constant velocity $V$ to the direction $O'X$.

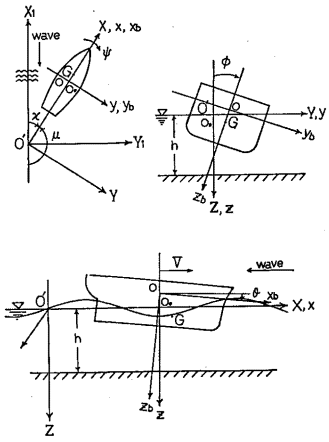


Fig. 2.2 Co-ordinate systems

Suppose that a ship operates with a constant forward speed $V$ making small motions in the direction $O'X$ at an angle $\chi$ to the direction of the incident waves in regular waves. The linear coupling equations for longitudinal motions and lateral motions in oblique waves can be expressed by new strip method respectively as follows.[10,11]

The equations for longitudinal motions:

$$\left.\begin{aligned}&(M+A_{33})\ddot{Z}+B_{33}\dot{Z}+C_{33}Z+A_{35}\ddot{\theta}+B_{35}\dot{\theta}+C_{35}\theta=F_{ze}\\&(J_{55}+A_{55})\ddot{\theta}+B_{55}\dot{\theta}+C_{55}\theta+A_{53}\ddot{Z}+B_{53}\dot{Z}+C_{53}Z=M_{\theta e}\end{aligned}\right] \tag{2.1}$$

where

$$\left[\begin{aligned}&A_{33}=\int_L M_H dx_b, \quad B_{33}=\int_L N_H dx_b, \quad C_{33}=\rho g A_w,\\&A_{35}=\int_L M_H\cdot x_b dx_b, \quad B_{35}=\int_L (N_H\cdot x_b-VM_H)dx_b, \quad C_{35}=\int_L (\rho g B_x\cdot x_b-VN_H)dx_b.\end{aligned}\right. \tag{2.2}$$

$$\left[\begin{array}{lll} A_{55}=\int_L M_H x_b^2 dx_b, & B_{55}=\int_L \left\{N_H x_b^2+\left(\frac{V}{\omega_e}\right)^2 N_H\right\} dx_b, & C_{35}=\int_L (\rho g B_x \cdot x_b^2 - V^2 M_H)\, dx_b, \\ A_{53}=A_{35}, & B_{53}=\int_L (N_H \cdot x_b + V M_H)\, dx_b, & C_{53}=\int_L (\rho g B_x \cdot x_b + V N_H)\, dx_b. \end{array}\right. \tag{2.3}$$

The wave exciting forces and moments are expressed as follows:

$$\left.\begin{array}{l} F_{ze}=F_{zc}\cos\omega_e t - F_{zs}\sin\omega_e t \\ M_{\theta e}=M_{\theta c}\cos\omega_e t - M_{\theta s}\sin\omega_e t \end{array}\right] \tag{2.4}$$

and the coefficient $F_{zc}$, $F_{zs}$, $M_{\theta c}$ and $M_{\theta s}$ are given as follows:

$$\begin{aligned} \left.\begin{array}{l} F_{zc} \\ F_{zs} \end{array}\right] &= \left[\begin{array}{c} - \\ + \end{array}\right] 2\rho g\zeta_a \int_L \left[\begin{array}{c} \cos \\ \sin \end{array}\right] (m_0 x_b \cos\mu) \int_0^b \frac{\cosh m_0(h-z_s)}{\cosh m_0 h} \cos(m_0 y_s \sin\mu)\, dy_s dx_b \\ &\left[\begin{array}{c} + \\ - \end{array}\right] \zeta_a \int_L \frac{\sinh m_0(h-T_m)}{\sinh m_0 h} \cdot \omega\omega_e M_H \left[\begin{array}{c} \cos \\ \sin \end{array}\right] (m_0 x_b \cos\mu)\, dx_b \\ &-\zeta_a \int_L \frac{\sinh m_0(h-T_m)}{\sinh m_0 h} \cdot \omega N_H \left[\begin{array}{c} \sin \\ \cos \end{array}\right] (m_0 x_b \cos\mu)\, dx_b. \end{aligned} \tag{2.5}$$

$$\begin{aligned} \left.\begin{array}{l} M_{\theta c} \\ M_{\theta s} \end{array}\right] &= \left[\begin{array}{c} - \\ + \end{array}\right] 2\rho g\zeta_a \int_L x_b \left[\begin{array}{c} \cos \\ \sin \end{array}\right] (m_0 x_b \cos\mu) \int_0^b \frac{\cosh m_0(h-z_s)}{\cosh m_0 h} \cos(m_0 y_s \sin\mu)\, dy_s dx_b \\ &\left[\begin{array}{c} + \\ - \end{array}\right] \zeta_a \int_L \frac{\sinh m_0(h-T_m)}{\sinh m_0 h} \left(\omega\omega_e M_H x_b - \frac{\omega}{\omega_e} V N_H\right) \left[\begin{array}{c} \cos \\ \sin \end{array}\right] (m_0 x_b \cos\mu)\, dx_b \\ &-\zeta_a \int_L \frac{\sinh m_0(h-T_m)}{\sinh m_0 h} (\omega N_H x_b + \omega V M_H) \left[\begin{array}{c} \sin \\ \cos \end{array}\right] (m_0 x_b \cos\mu)\, dx_b. \end{aligned} \tag{2.6}$$

The equations for lateral equations:

$$\left.\begin{array}{l} (M+A_{22})\ddot{y}+B_{22}\dot{y}+A_{26}\ddot{\psi}+B_{26}\dot{\psi}+A_{24}\ddot{\phi}+B_{24}\dot{\phi}=F_{ye} \\ (J_{44}+A_{44})\ddot{\phi}+B_{44}\dot{\phi}+C_{44}\phi+A_{42}\ddot{y}+B_{42}\dot{y}+A_{46}\ddot{\psi}+B_{46}\dot{\psi}=M_{\phi e} \\ (J_{66}+A_{66})\ddot{\psi}+B_{26}\dot{\psi}+A_{64}\ddot{\phi}+B_{64}\dot{\phi}+A_{62}\ddot{y}+B_{62}\dot{y}=M_{\psi e} \end{array}\right] \tag{2.7}$$

The coefficient $A_{ij}$, $B_{ij}$ and $C_{44}$ in equation (2.7) are given as follows:

$$\left\{\begin{array}{ll} A_{22}=\int_L M_s dx_b, & B_{22}=\int_L N_S dx_b, \\ A_{26}=\int_L M_S x_b dx_b + \frac{V}{\omega_e^2}\int_L N_S dx_b, & B_{26}=\int_L N_S x_b dx_b - V\int_L M_S dx_b, \\ A_{24}=\int_L M_S(\overline{OG}-l_{SR})\, dx_b, & B_{24}=\int_L N_S(\overline{OG}-l_\omega)\, dx_b. \end{array}\right. \tag{2.8}$$

$$\left\{\begin{aligned}
&A_{66}=\int_L M_S x_b^2 dx_b+\frac{V^2}{\omega_e^2}\int_L M_S dx_b, \qquad B_{66}=\int_L N_S x_b^2 dx_b+\frac{V^2}{\omega_e^2}\int_L N_S dx_b,\\
&A_{64}=\int_L M_S(\overline{OG}-l_{SR})x_b dx_b-\frac{V}{\omega_e^2}\int_L N_S(\overline{OG}-l_\omega)dx_b,\\
&B_{64}=\int_L N_S(\overline{OG}-l_\omega)x_b dx_b+V\int_L M_S(\overline{OG}-l_{SR})dx_b,\\
&A_{62}=\int_L M_S x_b dx_b-\frac{V}{\omega_e^2}\int_L N_S dx_b, \qquad B_{62}=\int_L N_S x_b dx_b+V\int_L M_S dx_b.
\end{aligned}\right. \tag{2.9}$$

$$\left\{\begin{aligned}
&A_{44}=\int_L M_S(l_{SR}l_{RS}-2\overline{OG}\cdot l_{SR}+\overline{OG}^2)dx_b,\\
&B_{44}=\int_L N_S(\overline{OG}-l_\omega)^2 dx_b, \qquad C_{44}=W\cdot\overline{GM},\\
&A_{42}=\int_L M_S(\overline{OG}-l_{SR})dx_b, \qquad B_{42}=\int_L N_S(\overline{OG}-l_w)dx_b,\\
&A_{46}=\int_L M_S(\overline{OG}-l_{SR})x_b dx_b+\frac{V}{\omega_e^2}\int_L N_S(\overline{OG}-l_w)dx_b,\\
&B_{46}=\int_L N_S(\overline{OG}-l_w)x_b dx_b-V\int_L M_S(\overline{OG}-l_{SR})dx_b.
\end{aligned}\right. \tag{2.10}$$

The wave exciting forces and moments are expressed as follows:

$$\left.\begin{aligned}
F_{ye} &= F_{yc}\cos\omega_e t - F_{ys}\sin\omega_e t\\
M_{\phi e} &= M_{\phi c}\cos\omega_e t - M_{\phi s}\sin\omega_e t\\
M_{\phi e} &= M_{\phi c}\cos\omega_e t - M_{\phi s}\sin\omega_e t
\end{aligned}\right\} \tag{2.11}$$

and the coefficients $F_{yc}, F_{ys}\cdots\cdots M_{\phi s}$ are given as follows:

$$\begin{aligned}
\begin{bmatrix}F_{yc}\\F_{ys}\end{bmatrix} &= -2\rho g\zeta_a\int_L\begin{bmatrix}\sin\\\cos\end{bmatrix}(m_0x_b\cos\mu)\int_0^T\frac{\cosh m_0(h-z_s)}{\cosh m_0h}\sin(m_0y_s\sin\mu)dz_s dx_b\\
&\quad -\zeta_a\sin\mu\int_L\omega\omega_e M_s\frac{\cosh m_0(h-T/2)}{\sinh m_0h}\begin{bmatrix}\sin\\\cos\end{bmatrix}(m_0x_b\cos\mu)dx_b\\
&\quad \begin{bmatrix}-\\+\end{bmatrix}\zeta_a\sin\mu\int_L\omega N_s\frac{\cosh m_0(h-T/2)}{\sinh m_0h}\begin{bmatrix}\cos\\\sin\end{bmatrix}(m_0x_b\cos\mu)dx_b.
\end{aligned} \tag{2.12}$$

$$\begin{aligned}
\begin{bmatrix}M_{\phi c}\\M_{\phi s}\end{bmatrix} &= \overline{OG}\cdot\begin{bmatrix}F_{yc}\\F_{ys}\end{bmatrix}\\
&\quad -2\rho g\zeta_a\int_L\begin{bmatrix}\sin\\\cos\end{bmatrix}(m_0x_b\cos\mu)\left\{\int_0^b\frac{\cosh m_0(h-z_s)}{\cosh m_0h}y_s\sin(m_0y_s\sin\mu)dy_s\right.
\end{aligned}$$

$$-\int_0^T \frac{\cosh m_0(h-z_s)}{\cosh m_0 h} z_s \sin(m_0 y_s \sin\mu)\, dz_s \Big\} dx_b$$

$$+\zeta_a \sin\mu \int_L \omega\omega_e M_s l_{sR} \frac{\cosh m_0(h-T/2)}{\sinh m_0 h} \begin{bmatrix} \sin \\ \cos \end{bmatrix} (m_0 x_b \cos\mu)\, dx_b$$

$$\begin{bmatrix} + \\ - \end{bmatrix} \zeta_a \sin\mu \int_L \omega N_s l_w \frac{\cosh m_0(h-T/2)}{\sinh m_0 h} \begin{bmatrix} \cos \\ \sin \end{bmatrix} (m_0 x_b \cos\mu)\, dx_b. \tag{2.13}$$

$$\begin{bmatrix} M_{\varphi c} \\ M_{\varphi s} \end{bmatrix} = -2\rho g \zeta_a \int_L x_b \begin{bmatrix} \sin \\ \cos \end{bmatrix} (m_0 x_b \cos\mu) \int_0^T \frac{\cosh m_0(h-z_s)}{\cosh m_0 h} \sin(m_0 y_s \sin\mu)\, dz_s dx_b$$

$$-\zeta_a \sin\mu \int_L \frac{\cosh m_0(h-T/2)}{\sinh m_0 h} \left(\omega\omega_e M_s x_b - \frac{\omega}{\omega_e} V N_s\right) \begin{bmatrix} \sin \\ \cos \end{bmatrix} (m_0 x_b \cos\mu)\, dx_b$$

$$\begin{bmatrix} - \\ + \end{bmatrix} \zeta_a \sin\mu \int_L \frac{\cosh m_0(h-T/2)}{\sinh m_0 h} (\omega N_s x_b + \omega V M_s) \begin{bmatrix} \cos \\ \sin \end{bmatrix} (m_0 x_b \cos\mu)\, dx_b. \tag{2.14}$$

where the origine of coordinate system fixed in the ship body is coincident with the center of gravity of the ship, and

$m_0$ : wave number in water of finite depth
(a real root of equation: $\frac{\omega^2}{g} = m_0 \tan m_0 h$)
$h$ : depth of water
$\omega_e$ : encounter circular frequency ($=\omega - m_0 V \cos\mu$)
$\zeta_a$ : amplitude of incident wave
$\rho$ : density of water
g : gravitational acceleration
$T_m$ : mean draft ($=S_x/B_x$)
$M_H, M_S$ : sectional added mass for heave and sway
$N_H, N_S$ : sectional damping force for heave and sway
$l_{SR}$ : lever of sectional added moment of inertia due to sway
$l_w$ : lever of sectional damping moment due to sway

In the next place, according to the relationship of Haskind-Newman-Bessho[12] the wave exciting forces and moments in the beam sea condition ($\mu=90°$) can be obtained precisely as follows:

$$\left.\begin{aligned} F_{ze} &= \int_L \frac{-i\rho g \zeta_a \hat{A}_H}{K \cdot F(m_0 h)} \cdot e^{i(\varepsilon_H + \omega t)} dx_b, \\ M_{\theta e} &= \int_L \frac{-i\rho g \zeta_a \hat{A}_H}{K \cdot F(m_0 h)} \cdot x_b e^{i(\varepsilon_H + \omega t)} dx_b. \end{aligned}\right\} \tag{2.15}$$

$$\left.\begin{aligned} F_{ye}&=\int_L \frac{-i\rho g\zeta_a \hat{A}_S}{K\cdot F(m_0h)}\cdot e^{i(\varepsilon_S+\omega t)}dx_b,\\ M_{\phi e}&=\overline{OG}\cdot F_{ye}+\int_L \frac{-i\rho g\zeta_a \hat{A}_R}{K\cdot F(m_0h)}T\cdot e^{i(\varepsilon_R+\omega t)}dx_b,\\ M_{\psi e}&=\int_L \frac{-i\rho g\zeta_a \hat{A}_S}{K\cdot F(m_0h)}x_b\cdot e^{i(\varepsilon_S+\omega t)}dx_b. \end{aligned}\right\} \qquad (2.16)$$

where

$$F(m_0h)=\frac{2\cosh^2 m_0h}{2m_0h+\sinh 2m_0h},\quad K=\frac{\omega^2}{g},$$

$\hat{A}_H, \hat{A}_S, \hat{A}_R$ : wave amplitude ratio for heave, sway and roll,
$\varepsilon_H, \varepsilon_S, \varepsilon_R$ : phase lag for heave, sway and roll.

## 2.2 Effects of water depths for hydrodynamic coefficients

The hydrodynamic coefficient $A_{ij}, B_{ij}, C_{ij}$ of the left hand of equations (2.1) and (2.7) represent the inertia terms, the damping terms and the restoring terms respectively. And the subscript $i$ expresses the oscillating mode as, $i=2$: swaying mode, $i=3$: heaving mode, $i=4$: rolling mode, $i=5$: pitching mode and $i=6$: yawing mode.

The effects of water depths for these coefficients are shown in Fig. 2.3 ~Fig. 2.22. The non-dimensional expressions of these coefficients are shown as follows.

Non-dimensional coefficients of the equations for longitudinal motions
(a) Heave

$$\hat{M}+\hat{A}_{33}=\frac{M+A_{33}}{\rho L^3},\qquad \hat{B}_{33}=\frac{B_{33}}{\rho L^3}\sqrt{L/g},$$

$$\hat{A}_{53}=\frac{A_{53}-C_{53}/\omega^3}{\rho L^4},\qquad \hat{B}_{53}=\frac{B_{53}}{\rho L^4}\sqrt{L/g}.$$

(b) Pitch

$$\hat{J}_{55}+\hat{A}_{55}=\frac{J_{55}+A_{55}}{\rho L^5},\qquad \hat{B}_{55}=\frac{B_{55}}{\rho L^5}\sqrt{B/2g},$$

$$\hat{A}_{35}=\frac{A_{35}-C_{35}/\omega^2}{\rho L^4},\qquad \hat{B}_{35}=\frac{B_{35}}{\rho L^4}\sqrt{B/2g}.$$

Non-dimensional coefficients of the equations for lateral motions
(a) Sway

$$\hat{M}+\hat{A}_{22}=\frac{M+A_{22}}{M}, \qquad \hat{B}_{22}=\frac{B_{22}}{M}\sqrt{B/2g},$$

$$\hat{A}_{42}=\frac{A_{42}}{M\cdot B}, \qquad \hat{B}_{42}=\frac{B_{42}}{M\cdot B}\sqrt{B/2g},$$

$$\hat{A}_{62}=\frac{A_{62}}{M\cdot L}, \qquad \hat{B}_{62}=\frac{B_{62}}{M\cdot L}\sqrt{B/2g},$$

(b) Roll

$$\hat{J}_{44}+\hat{A}_{44}=\frac{J_{44}+A_{44}}{M\cdot B^2}, \qquad \hat{B}_{44}=\frac{B_{44}}{M\cdot B^2}\sqrt{B/2g},$$

$$\hat{A}_{24}=\frac{A_{24}}{M\cdot B}, \qquad \hat{B}_{24}=\frac{B_{24}}{M\cdot B}\sqrt{B/2g},$$

$$\hat{A}_{64}=\frac{A_{64}}{M\cdot L\cdot B}, \qquad \hat{B}_{64}=\frac{B_{64}}{M\cdot L\cdot B}\sqrt{B/2g},$$

(c) Yaw

$$\hat{J}_{66}+\hat{A}_{66}=\frac{J_{66}+A_{66}}{M\cdot L^2}, \qquad \hat{B}_{66}=\frac{B_{66}}{M\cdot L^2}\sqrt{B/2g},$$

$$\hat{A}_{26}=\frac{A_{26}}{M\cdot L}, \qquad \hat{B}_{26}=\frac{B_{26}}{M\cdot L}\sqrt{B/2g},$$

$$\hat{A}_{46}=\frac{A_{46}}{M\cdot L\cdot B}, \qquad \hat{B}_{46}=\frac{B_{46}}{M\cdot L\cdot B}\sqrt{B/2g}.$$

where

$L$: length of ship,
$B$: breadth of ship,
$M$: mass of ship, $(=\rho\Delta)$,
$\Delta$: displacement of ship,
$J_{ii}$: mass moment of inertia of ship for the $i$-th mode,
$\rho$: dencity of water,
$g$: gravitational acceleration.

### 2.2.1 Longitudinal motions

(i) Inertia terms : $\hat{A}_{33}, \hat{A}_{55}$

Both inertia terms $\hat{A}_{33}, \hat{A}_{55}$ for heaving and pitching increase very much at overall range of frequency as depths of water become more shallow shown in Fig. 2.3 and 2.4. The inertia terms in water of infinite depth increase infinitely in very low frequencies, while those in waters of finite depths yield a finite value respectively as a frequency becomes to zero ($\omega\rightarrow 0$).

(ii) Damping terms : $\hat{B}_{33}, \hat{B}_{55}$

Both damping terms $\hat{B}_{33}, \hat{B}_{55}$ increase very much at overall range of frequency as depths of water become more shallow shown in Fig. 2.5 and 2.6. Because the wave amplitude ratios $\hat{A}_H$ rapidly become larger in very low frequencies as the depths of water become more shallow (Fig. 2.5). The

above tendency is very different from that of the three dimensional calculated values.[6] $\hat{B}_{55}$ increses a little due to effects of a forward speed of a ship in low frequencies.

(iii) Restoring terms: $\hat{C}_{33}, \hat{C}_{55}$

The restoring term for heaving $\hat{C}_{33}$ without a forward speed is not affected by effects of water depths. The restoring term for pitching $\hat{C}_{55}$ is not affected due to effects of the water depths in the case of no forward speed, but has a tendency to decrease slightly the restoring moment as the depths of water become more shallow in the case of a forward speed.

(iv) Cross coupling term

When a ship has no forward speed: $V=0$, there exist the following symmetric relationship among the cross coupling terms obtained by new strip method:

$$\hat{B}_{35}=\hat{B}_{53},\quad \hat{C}_{35}=\hat{C}_{53},$$

whether $V=0$ or $V\neq 0$, there is the following symmetric relationship

$$\hat{A}_{35}=\hat{A}_{53}.$$

$\hat{A}_{35}=\hat{A}_{53}$ : The cross coupling terms $\hat{A}_{35}=\hat{A}_{53}$ which have a symmetric relationship increase as the depths of water become more shallow in Fig. 2.7.

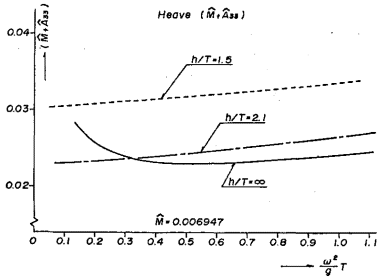


Fig. 2.3 $\hat{M}+\hat{A}_{33}$: Virtual mass coeff. for heave

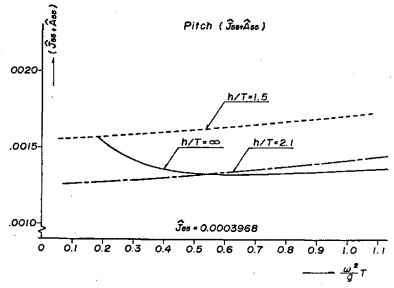


Fg. 2.4 $\hat{J}_{55}+\hat{A}_{55}$: Virtual mass moment of inertia coeff. for pitch

$\hat{B}_{35}$, $\hat{B}_{53}$ : The terms $\hat{B}_{35}=\hat{B}_{53}$ with no forward speed are not affected very much due to effects of water depths. In the case with forward speed, the term $\hat{B}_{35}$ decreases while the term $\hat{B}_{53}$ increases as the depths of water become more shallow shown in Fig. 2.8.

$\hat{C}_{35}$, $C_{53}$ : The terms $\hat{C}_{35}=\hat{C}_{53}$ with no forward speed are not affected due to effects of water depths. In the case with forward speed, $\hat{C}_{35}$ decreases and $\hat{C}_{53}$ increases conversely as depths of water become more shallow shown in Fig. 2.9.

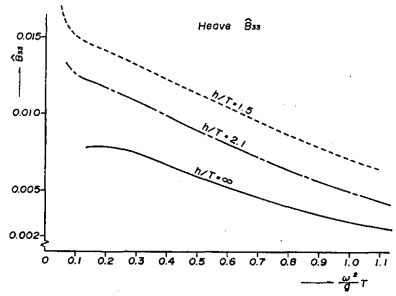


Fig. 2.5 $\hat{B}_{33}$: Damping force coeff. for heave

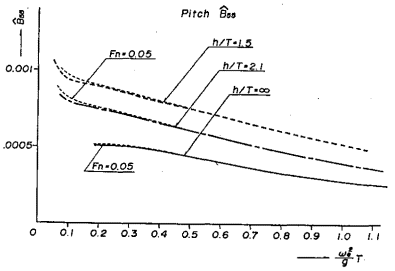


Fig. 2.6 $\hat{B}_{55}$: Damping moment coeff. for pitch

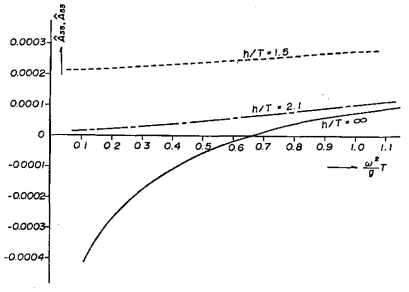


Fig. 2.7 $\hat{A}_{35}=\hat{A}_{53}$: Coupling term coeff. between heave and pitch

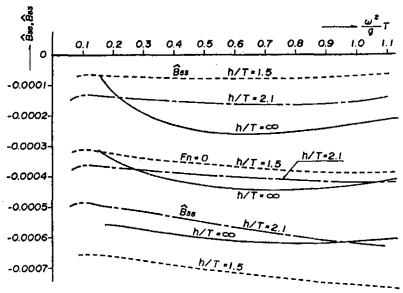


Fig. 2.8 $\hat{B}_{35}, \hat{B}_{53}$: Coupling term coeff. between heave and pitch

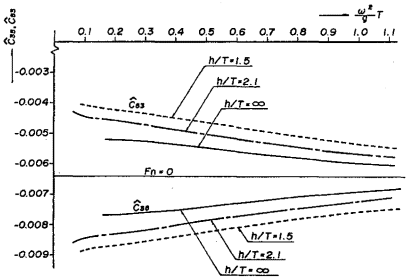


Fig. 2.9 $\hat{C}_{35}$, $\hat{C}_{53}$: Coupling term coeff. between heave and pitch

### 2.2.2 Lateral motions

(i) Principal terms of swaying: $\hat{A}_{22}$, $\hat{B}_{22}$

The added mass coefficients $\hat{A}_{22}$ decrease except for ones at very low frequencies as the depths of water become more shallow shown in Fig. 2.10.

The damping force coefficients $\hat{B}_{22}$ increase in low frequencies and decrease conversely in high frequencies as the depths of water become more

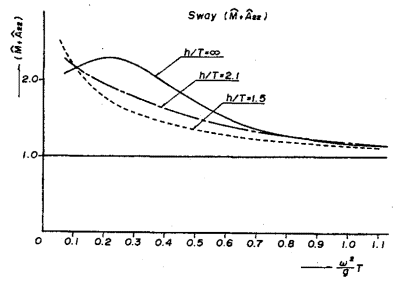


Fig. 2.10 $\hat{M}+\hat{A}_{22}$: Virtual mass coeff. for sway

shallow as shown in Fig. 2.11.

(ii) Principal terms of yawing: $\hat{A}_{66}$, $\hat{B}_{66}$

In the case with no forward speed, the principal terms of yawing $\hat{A}_{66}$, $\hat{B}_{66}$ have the same effects of water depths as those of principal terms of sway respectively. In the case with forward speed the principal terms increase slightly due to the effects of the forward speed respectively in low frequencies shown in Fig. 2.12 and Fig. 2.13.

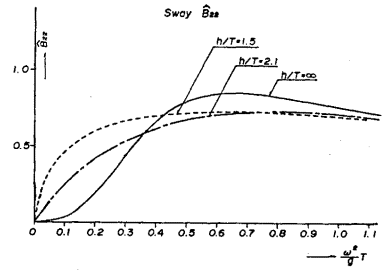


Fig. 2.11 $\hat{B}_{22}$: Damping for coeff. for sway

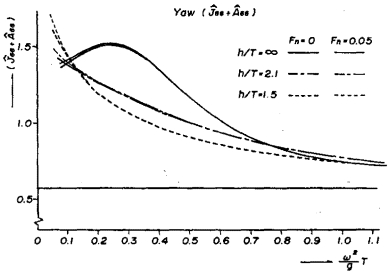


Fig. 2.12 $\hat{J}_{66}+\hat{A}_{66}$: Virtual mass moment of inertia coeff. for yaw

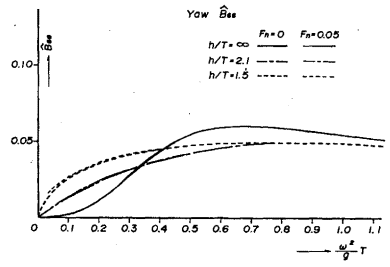


Fig. 2.13 $\hat{B}_{66}$: Damping moment coeff. for yaw

(iii) Added mass moment of inertia coefficient: $\hat{A}_{44}$

Added mass moment of inertia coefficients $\hat{A}_{44}$ acting on this ship model are scarcely affected by effect of water bottom in these water depths ($h/T=1.5,\ 2.1$) at overall frequencies shown in Fig. 2.14.

(iv) Damping moment coefficient for rolling: $\hat{B}_{44}$

According to the potential theory the damping moment coefficients $\hat{B}_{44}$ for rolling are completely composed of the wave damping moment. Actually the damping moment coefficients $\hat{B}_{44}$ for roll, however, depend on non-linear effects of the viscousness of fluid etc., and we cannot estimate rolling damping coefficient by adopting potential theory. So we have obtained the damping moment coefficients $\hat{B}_{44}$ of rolling by the free oscillating tests for rolling in still waters with finite depths as follows.

Suppose equation of a free oscillation about a center of gravity of a ship body $G$ can be expressed as follows:

$$(J_{44}+A_{44})\ddot{\phi}+B_1\dot{\phi}+B_2\dot{\phi}|\dot{\phi}|+C_{44}\phi=0 \tag{2.17}$$

where, $C_{44}=W\cdot\overline{GM}$,

and we put

$$2\alpha=\frac{B_1}{J_{44}+A_{44}},\quad \beta=\frac{B_2}{J_{44}+A_{44}}. \tag{2.18}$$

On the other hand, we express equation of extinction curves obtained by free oscillating tests for rolling as follows

$$\Delta\phi_n=a\phi_m+b\phi_m^2. \tag{2.19}$$

With aid of the relationship between the amount of work and the energy which is performed for one cycle by a free oscillating test for rolling, following equation can be obtained

$$\Delta\phi_n=\frac{B_1\pi^2}{W\cdot\overline{GM}\cdot T_\phi}\phi_m+\frac{16B_2\pi^2}{3T_\phi^2\cdot W\cdot\overline{GM}}\phi_m^2, \tag{2.20}$$

where, $T_\phi$: natural period of rolling

$$\phi_m=(\phi_n+\phi_{n+1})/2,\quad \Delta\phi_n=\phi_{n+1}-\phi_n\ \text{(degree)}.$$

and we can obtain the following relationships:

$$a=\frac{T_\phi}{2}\alpha,\quad b=\frac{4}{3}\beta,\quad B_1=\frac{2W\cdot\overline{GM}}{\pi\omega}a,\quad B_2=\frac{3W\cdot\overline{GM}}{4\omega^2}\frac{180}{\pi}b, \tag{2.21}$$

where, $\omega=2\pi/T_\phi$.

Substituting the damping terms of equation (2.17) for the equivalent linear damping, we have

$$B_1\dot{\phi}+B_2\dot{\phi}|\dot{\phi}| \doteqdot \left(B_1+\frac{8}{3\pi}\omega\phi_A \cdot B_2\right)\dot{\phi}$$

$$=B_{44}\dot{\phi}.$$

($\phi_A$: radian). (2.22)

It has been seen that a damping moment coefficient of rolling obtained by forced oscillation test can be represented very well by the expression of equation (2.22) in water of infinite depth.[13] Then suppose that we can express the damping moment coefficient of rolling due to above equation (2.22) in waters of finite depths, we have estimated the damping moment coefficient $\hat{B}_{44}$ for rolling by using the coefficients $a$ and $b$ which have been obtained from the extinction curve of the free oscillation test for rolling.

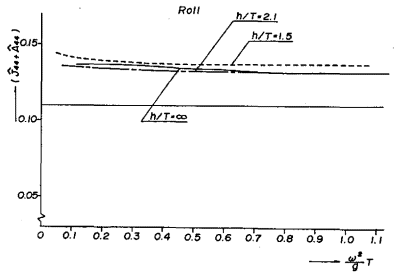


Fig. 2.14 $\hat{J}_{44}+\hat{A}_{44}$: Virtual mass moment of inertia coeff. for roll

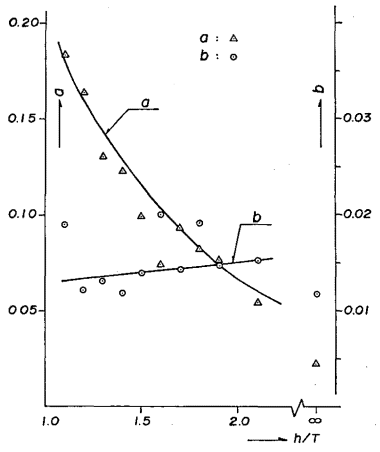


Fig. 2.15 Coeff. of extinction curves for free rolling at $Fn=0$

Fig. 2.15 shows the coefficients $a$, $b$ of the extinction curves obtained by using the values of the rolling amplitudes $\phi_A=3°$ and $5°$ with no forward speed ($F_n=0$) and the mean lines of these coefficients taking the ratios of the water depths and the draft of ship as the horizontal axis. And Table 2.2 shows the non-dimensional coefficients $\hat{B}_1, \hat{B}_2$ expressed as follows

$$\hat{B}_1=B_1\sqrt{B/2g}/\rho\Delta B^2, \quad \hat{B}_2=B_2/\rho\Delta B^2 \tag{2.23}$$

The values of $\hat{B}_1$ and $\hat{B}_2$ of the ore-carrier named Kasagisanmaru ($C_B=0.8243$) obtained by the forced oscillating test in water of infinite depth are shown in the same table for reference. It is seen from this table that the linear terms of the damping moment coefficient $\hat{B}_1$ increase rapidly as the depths of water become more shallow. The experimental values of those with forward speed ($F_n=0.05$) have a small difference from those with no forward speed above mentioned. As shown in Fig. 2.16, the natural periods of rolling oscillation increase rapidly at very shallow water ($h/T\leqq 1.4$) because of effects of water bottom.

Table 2.2 Damping moment coeff. for roll at $F_n=0$

| | $h/T$ | $a$ | $b$ | $\hat{B}_1$ | $\hat{B}_2$ | $T_\phi$ (sec) |
|---|---|---|---|---|---|---|
| S.R.-154 | | | | | | |
| Tanker ship model | 1.5 | 0.099 | 0.014 | 0.00533 | 0.08455 | 1.666 |
| ($C_B=0.82$) | 2.1 | 0.054 | 0.015 | 0.00282 | 0.08480 | 1.614 |
| | $\infty$ | 0.024 | 0.012 | 0.00121 | 0.06245 | 1.560 |
| Ore-carrier* | | | | | | |
| Kasagisanmaru | $\infty$ | — | — | 0.00193 | 0.05667 | 1.405 |
| ($C_B=0.8243$) | | | | | | |

* the values obtained by forced rolling test in deep water

(v) Cross coupling terms

When a ship has no forward speed: $V=0$, there exist the following symmetric relationships among the cross coupling terms obtained by new strip method as:

$$\hat{A}_{26}=\hat{A}_{62}, \quad \hat{B}_{26}=\hat{B}_{62}, \quad \hat{A}_{46}=\hat{A}_{64}, \quad \hat{B}_{46}=\hat{B}_{64},$$

whether $V=0$ or $V\neq 0$, there are the following symmetric relationships

$$\hat{A}_{24}=\hat{A}_{42}, \quad \hat{B}_{24}=\hat{B}_{42}.$$

$\hat{A}_{24}=\hat{A}_{42}$ : The cross coupling terms $\hat{A}_{24}=\hat{A}_{42}$ which have a symmetric relationship become larger in low frequencies as the depths of water become more shallow as shown in Fig. 2.17.

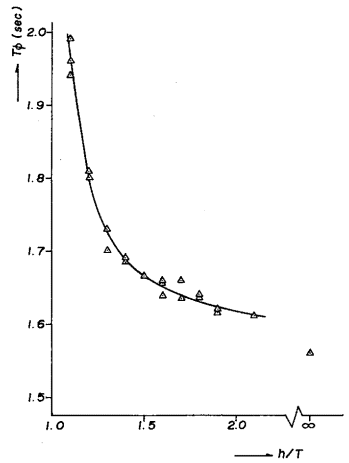


Fig. 2.16 Natural periods of free rolling at $Fn=0$

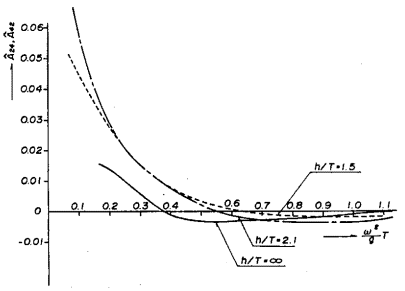


Fig. 2.17 $\hat{A}_{24}=\hat{A}_{42}$: Coupling term coeff. between sway and roll

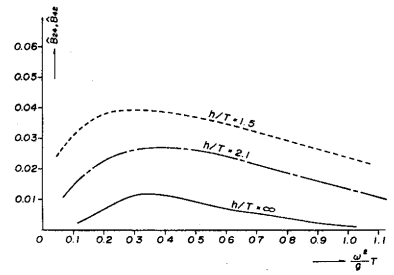


Fig. 2.18 $\hat{B}_{24}=\hat{B}_{42}$: Coupling term coeff. between sway and roll

$\hat{B}_{24}=\hat{B}_{42}$ : The cross coupling terms $\hat{B}_{24}=\hat{B}_{42}$ which have a symmetric relationship increase very much at overall frequencies as the depths of water become more shallow as shown in Fig. 2.18.

$\hat{A}_{26}, \hat{A}_{62}$ : When a ship has no forward speed, the cross coupling terms $\hat{A}_{26}$ and $\hat{A}_{62}$ decrease in low frequencies and increase in high frequencies as the depths of water become more shallow. When a ship has the forward speed ($F_n=0.05$), the term $\hat{A}_{26}$ is larger than that with no forward speed, and the term $\hat{A}_{62}$ is conversely smaller than that with zero-forward speed as shown in Fig. 2.19.

$\hat{B}_{26}, \hat{B}_{62}$ : The cross coupling terms $\hat{B}_{26}$ and $\hat{B}_{62}$ with no forward speed decrease except for ones at low frequencies as the depths of water become more shallow as shown in Fig. 2.20. When a ship has the forward speed ($F_n=0.05$), the term $\hat{B}_{26}$ is smaller and the term $\hat{B}_{62}$ is conversely larger than that with zero-forward speed respectively.

$\hat{A}_{46}, \hat{A}_{64}$ : The absolute values of the cross terms $\hat{A}_{46}$ and $\hat{A}_{64}$ with no forward speed become smaller as the depths of water become more shallow shown in Fig. 2.21. When a ship has a forward speed, the term $\hat{A}_{46}$ increase and the term $\hat{A}_{64}$ decrease due to the effects of a forward speed. These effects of forward speed affect

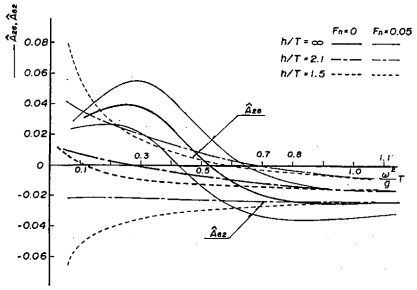


Fig. 2.19 $\hat{A}_{26}, \hat{A}_{62}$: Coupling term coeff. between sway and yaw

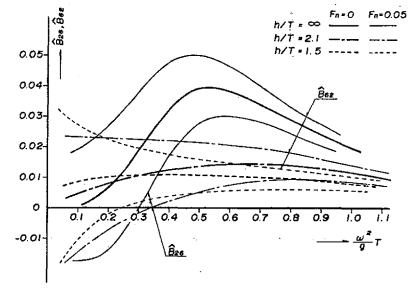


Fig. 2.20 $\hat{B}_{26}, \hat{B}_{62}$: Coupling term coeff. between sway and yaw

strongly on the values of $\hat{A}_{46}$ and $\hat{A}_{64}$ in low frequencies as the depths of water become more shallow.

$\hat{B}_{46}, \hat{B}_{64}$ : As shown in Fig. 2.22, the absolute values of the cross terms $\hat{B}_{46}$ and $\hat{B}_{64}$ with no forward speed in waters of finite depths are smaller than that of in finitely deep water respectively. In the case with the forward speed $F_{\infty}=0.05$, the term $\hat{B}_{46}$ decrease slightly and the term $\hat{B}_{64}$ increases slightly in low frequencies.

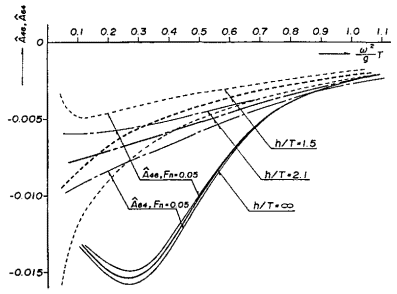


Fig. 2.21 $\hat{A}_{46}$, , $\hat{A}_{64}$: Coupling term coeff. between roll and yaw

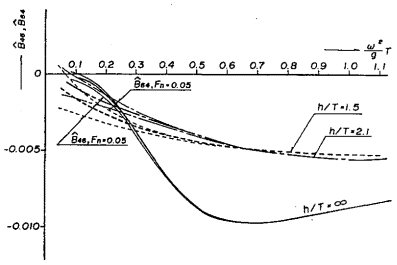


Fig. 2.22 $\hat{B}_{46}, \hat{B}_{64}$: Coupling term coeff. between roll and yaw

## 2.3 Effects of water depths for wave exciting forces and moments

The non-dimensional expressions of the forces and moments acting on the ship are shown as follows:

wave exciting force for sway : $\hat{F}_y = |F_{ye}| / \rho g \zeta_a L^2$
wave exciting force for heave : $\hat{F}_z = |F_{ze}| / \rho g \zeta_a L^2$
wave exciting moment for roll : $\hat{M}_\phi = |M_{\phi e}| / \rho g \zeta_a L^3$
wave exciting moment for pitch : $\hat{M}_\theta = |M_{\theta e}| / \rho g \zeta_a L^3$
wave exciting moment for yaw : $\hat{M}_\phi = |M_{\phi e}| / \rho g \zeta_a L^3$

The numerical calculations of these forces and moments are carried out in accordance with the experimental conditions shown in Table 3.1. These numerical results are shown in Fig. 2.23～ Fig. 2.29.

Table 3.1 Experimental conditions

| Conditions | $F_n$ Ship speed | $h/T$ Water depth | Periods of wave |
|---|---|---|---|
| Head sea ($\mu$=180°) | 0, 0.05 | 1.5, 2.1 | $T_W$=0.8~1.9 (sec) |
| Bow sea ($\mu$=135°) | 0, 0.05 | 1.5, 2.1 | |
| Beam sea ($\mu$= 90°) | 0 | 1.5 | |
| Following sea ($\mu$= 0°) | 0, 0.05 | 1.5 | |
| | 0 | 2.1 | |

(i) Heaving forces: $\hat{F}_z$

Fig. 2.23 shows the wave exciting heaving forces with no forward speed in various heading angles. The values of heaving forces in beam sea condition increase at overall frequencies as depths of water become more shallow. The tendencies of effects of water bottom on the wave exciting heaving forces in head sea, bow sea and following sea condition agree well, namely the heaving forces decrease in low frequencies as the depths of water become more shallow. As shown in Fig. 2.24 the tendencies of effects of water bottom on the heaving forces with forward speed ($F_n$=0.05) are similar to those with zero-forward speed except for ones in beam sea condition. The heaving forces in bow sea condition are slightly larger than ones in head sea and following sea conditions in low frequencies.

(ii) Pitching moments: $\hat{M}_\theta$

Fig. 2.25 shows the wave exciting pitching moments with no forward speed in various heading angles. The pitching moments in beam sea condition are the smallest values and those in head sea and following sea condition are the largest values, which take a figure up one place. The maximum peaks of the pitching moments in head sea condition become larger in low frequencies as the depths of water become more shallow. The above tendency can be seen in bow sea condition and following sea condition. Fig. 2.26 shows the pitching moments with the forward speed ($F_n$=0.05), of which tendencies are in the same as those with zero-forward speed above mentioned.

(iii) Swaying forces: $\hat{F}_y$

The wave exciting swaying forces in beam sea and bow sea conditions are shown in Fig. 2.27. The swaying forces in beam sea condition increase rapidly in low frequencies as the depths of water become more shallow. The depths of water, however, does not affect strongly the values of swaying forces in high frequencies.

In bow sea condition the wave exciting swaying forces increase in low frequencies and decrease conversely in high frequencies as the depths of water become more shallow. This tendency of effects of water bottom on

the wave exciting swaying forces with no forward speed can be seen similarly in case with the forward speed $F_n=0.05$.

(iv) Rolling moments: $\hat{M}_\phi$

Fig. 2.28 shows the wave exciting rolling moments in beam sea and bow sea conditions. The rolling moments in beam sea condition increase very much at overall frequencies as depths of water become more shallow. The wave exciting rolling moments in bow sea conditions are smaller than those in beam sea condition. The maximum peaks of those in waters of finite depths, however, are larger than that of infinitely deep water. There are a few frequencies where the wave exciting rolling moments in waters of finite depths are zero in our numerical results.

(v) Yaw moments: $\hat{M}_\psi$

Fig. 2.29 shows the wave exciting yawing moments in beam sea and bow sea conditions. Since the yawing moments are generated due to asymmetric ship forms of fore and aft in beam sea condition, the values of yawing moments acting on the tanker ship model are very small. The order of the values of yawing moments in bow sea condition is larger by taking a figure up on place than ones in beam sea condition. In the bow sea condition, the wave exciting moments of yawing increase in low frequencies and conversely decrease in high frequencies as the depths of water become more shallow whether the ship has zero-forward speed or the forward speed ($F_n=0.05$).

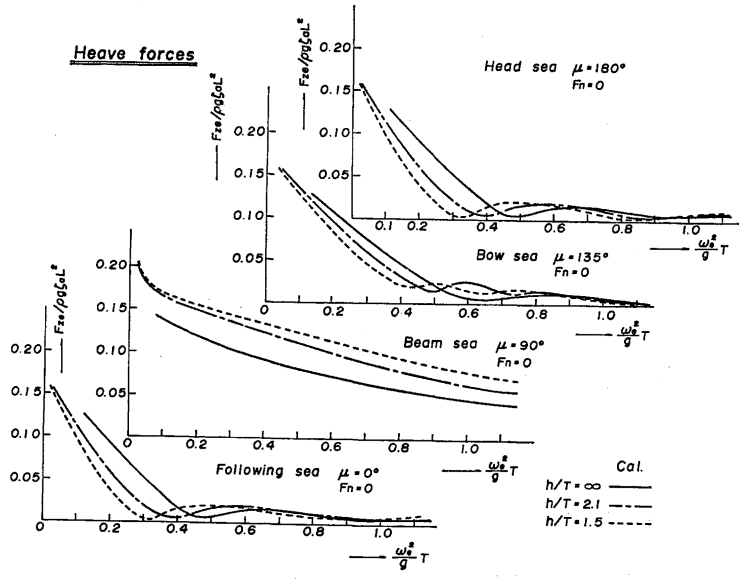


Fig. 2.23 Wave exciting forces for heave at $Fn=0$ in various heading angles

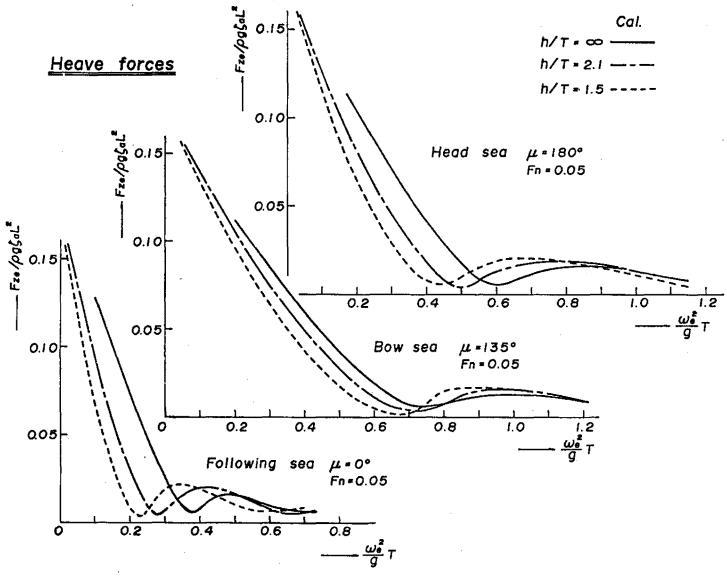


Fig. 2.24 Wave exciting forces for heave at $Fn=0.05$ in various heading angles

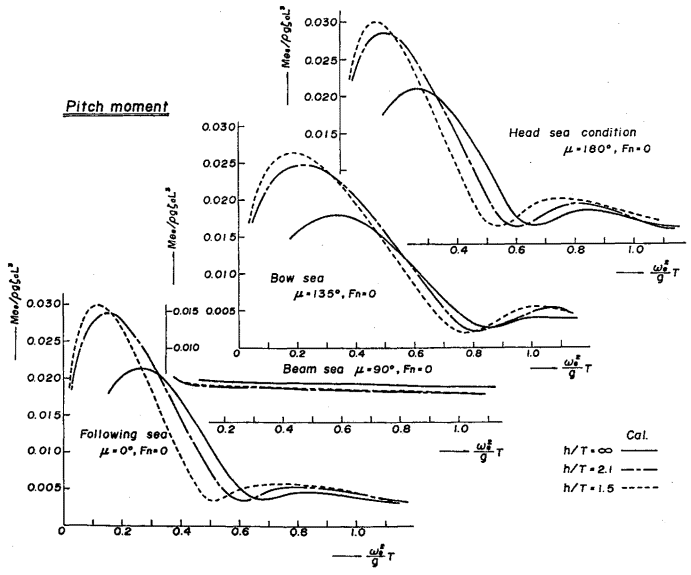


Fig. 2.25 Wave exciting moments for pitch at $Fn=0$ in various heading angles

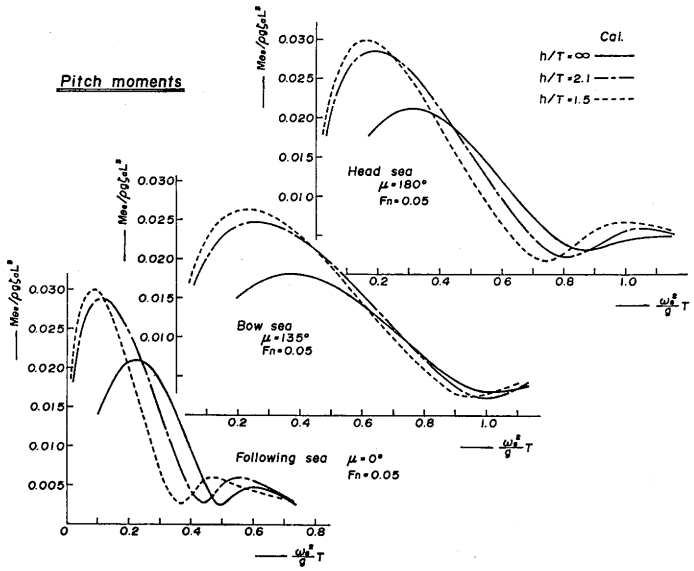


Fig. 2.26 Wave exciting moments for pitch at $Fn=0.05$ in various heading angles

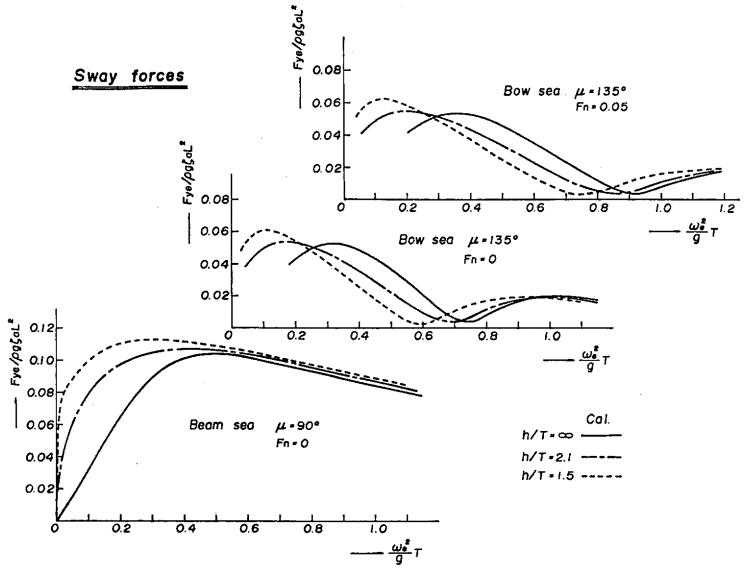


Fig. 2.27 Wave exciting forces for sway in various heading angles

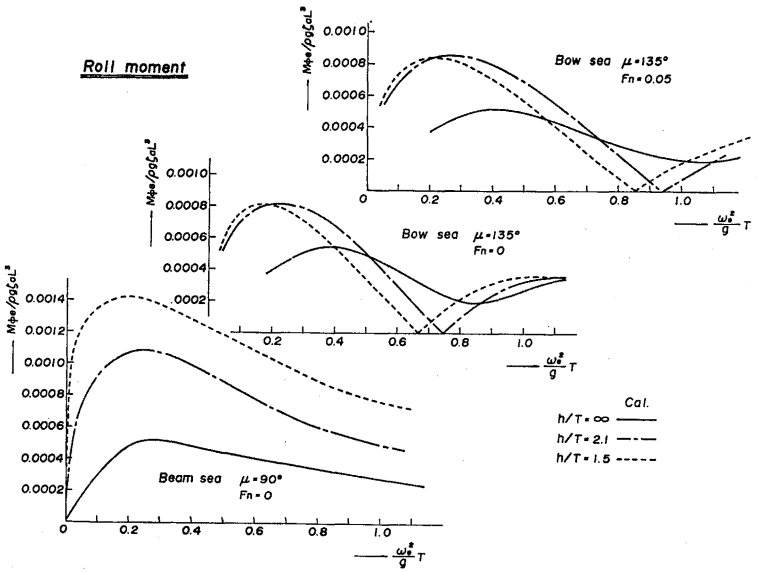


Fig. 2.28 Wave exciting moments for roll in various heading angles

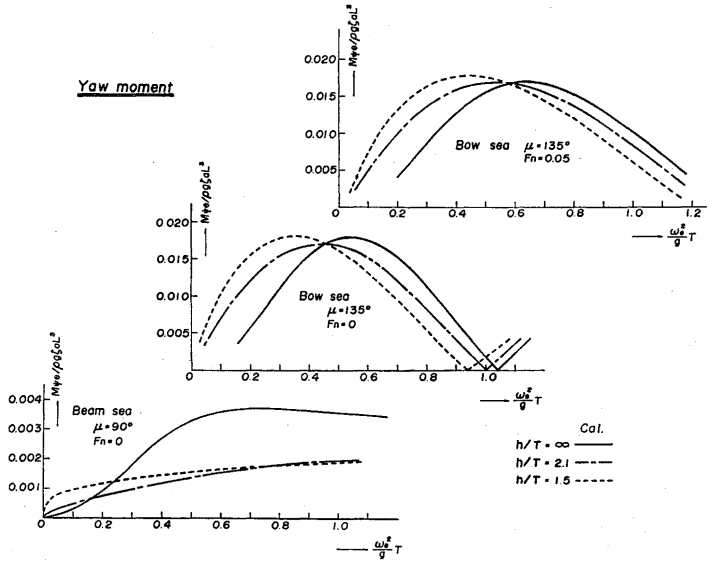


Fig. 2.29 Wave exciting moments for yaw in various heading angles

## 3. Experiments of ship motions in oblique waves

The experiments of ship motions were performed at the Seakeeping and Manoeuvering Tank of Department of Naval Architecture in Kyushu University. Table 3.1 shows the experimental conditions which have two kinds of water depths, two kinds of ship speeds and four kinds of heading angles.

We measured the displacements of five modes which were heaving, pitching, swaying, rolling and yawing amplitudes. Heaving displacement was measured by means of accelerometer of strain gauge type, and swaying displacement was measured by means of synchronical accelerometer, and pitching and rolling amplitude were measured by means of virtical gyro meter, and yawing amplitude was measured by means of rate gyro meter as shown in Fig. 3.1. These measuring instruments were equiped in the ship model and the operations of these instruments were carried out by means of radio. The forward speed of the ship was determined by measuring the time when the ship operated between two marks in the tank. Since the drifting force acting on the ship with a forward speed in beam sea condition was very strong and the ship's course was very unstable in its condition, we could not measure the amplitudes of motions of the ship model with forward speed in its condition.

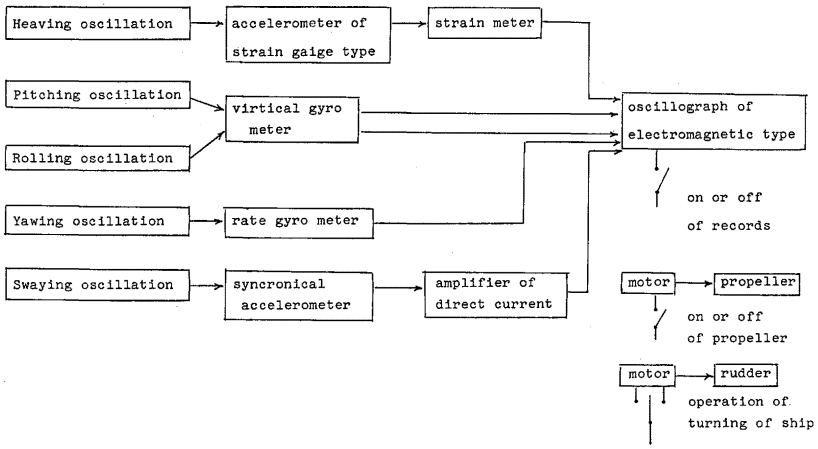


Fig. 3.1 Arrangement of measuring instruments in experiments

## 4. Comparison of the experimental results with the numerical ones

We have solved the coupled equations of ship motions (2.1) and (2.7) by using the damping coefficient $\hat{B}_{44}$ for roll obtained by the free oscillating tests and compared the numerical results with the experimental ones. These correlation works are shown in Fig. 4.1~Fig. 4.7 taking non-dimen-

sional frequency ($\frac{\omega^2_e}{g}T$) as the horizontal axis and the amplitudes of ship motions in water of infinite depth also are shown in same figures for reference.

(i) Heaving amplitudes

Fig. 4.1 shows the heaving amplitudes with zero-advancing speed in various heading angles. In beam sea condition ($\mu=90°$) the resonant peaks of the heaving motions appear and the amplitudes of resonance are about 1.5 times as large as the wave amplitude. The resonant peak shifts largely to low frequencies as the depths of water become more shallow, because the added mass for heaving oscillation increase largely as the depths of water become more shallow. Hence it is seen from the above results that the effects of water depths affect strongly the virtical motions. The theoretically calculated results and the experimental ones agree almost in beam sea condition.

In the next place, the heaving amplitudes in head sea condition become smaller in low frequencies as the depths of water become more shallow. These tendencies above mentioned are similarly appeared in heaving amplitudes in bow sea condition and following sea condition. The theoretically calculated results of heaving amplitudes agree qualitatively with the experimental results, but does not agree quantitatively with the experimental results in especially low frequencies, where the experimental results of heaving amplitudes are larger than the numerical results. It seems that these causes are originated due to the experimental and the analytical errors, because the wave amplitudes generated at the shallow water tank were very small in low frequencies and the displacements of heaving motions were measured as the heaving accelerations by means of accelerometer and these accelerations were transformed to the heaving displacements by the two times of integrations. Beck and Tuck explained according to the comparison with Kim's results obtained by strip theory in shallow water that slender body theory seemed to give more accetable results in low frequencies, while strip theory should be more accurate in high frequencies[5]. It seems that their opinions are reasonable according to Fig. 4.1 and Fig. 4.2. However as to pitching motions which shall be discussed in next section, the pitching amplitudes coupled to the heaving motions are estimated precisely by the new strip method. It is necessary to study about these results hereafter.

Fig. 4.2 shows the heaving amplitudes with the forward speed $F_n=0.05$ in various heading angles. The experimental results of heaving amplitudes with a forward speed in range of low frequency are also larger than the numerical results in all conditions. But in range of high frequency the theoretical calculations and the experimental results of heaving amplitudes agree very well whether the ship has an advancing speed or not.

(ii) Pitching amplitudes

The pitching amplitudes with zero-advancing speed and with the advancing

speed in various heading angles are shown in Fig. 4.3 and Fig. 4.4 respectively. The pitching amplitudes are more precisely estimated than the heaving amplitudes as mentioned in previous section and the theoretical calculations of pitching amplitudes are in fair good agreement with the experimental results whether the advancing speed is equal to zero or not. Because since the pitching motions have been measured by means of the virtical gyro meter, it seems that there is little experimental and analytical error. The pitching amplitudes become smaller as the depths of water become more shallow in head sea, following sea and bow sea conditions. In beam sea condition the pitching amplitudes are smaller by taking a figure down one place than those in other conditions but have a resonance peak in each depth of water. This resonance peak shifts to the range of low frequency as the depths of water become more shallow in the same tendency as the heaving amplitudes in beam sea condition.

(iii) Swaying amplitudes

Fig. 4.5 shows the swaying amplitudes in beam sea and bow sea conditions. Now it is the most interesting thing that the swaying amplitudes increase rapidly and become larger than the wave amplitude in the range of low frequency. Especially the swaying amplitudes in beam sea condition are larger than two times of the wave amplitude in low frequencies. Because the horizontal fluid particle motion are larger than the virtical fluid particle motion at all frequency in waters of finite depths. Since the swaying motion affects significantly the tensions of mooring lines of a ship moored, it is necessary to take care of mooring a ship in shallow water. In beam sea condition theoretical calculations of swaying amplitudes are in fair good agreement with the experimental results. The swaying amplitudes increase at overall frequencies as the depths of water become more shallow. On the other hand in bow sea conditions experimental results of swaying amplitudes yield higher values than the numerical results in the range of low frequency. The numerical results of swaying amplitudes however agree qualitatively with the experimental results. The swaying amplitudes increase in the range of low frequency and conversely decrease in the range of middle frequency ($0.3 \leqq \frac{\omega^2_e}{g} T \leqq 0.6$) as the depths of water become shallow.

(iv) Rolling amplitudes

Fig. 4.6 shows the rolling amplitudes in beam sea and bow sea conditions. In beam sea condition the theoretical calculations and the experimental results of rolling amplitudes agree very well. The rolling amplitudes are scarcely affected except for those at resonant frequency by the effects of water depth. The resonant peaks of rolling amplitudes become larger as the depths of water become more shallow, because the wave exciting moments for rolling become larger as the depths of water become more shallow shown in Fig. 2.28. But since the damping moment coefficients $\hat{B}_{44}$ also increase as

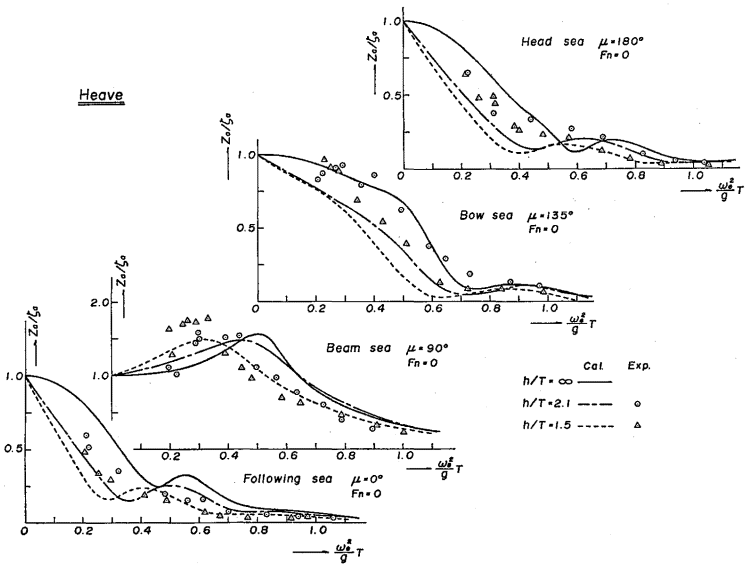


Fig. 4.1 Heaving amplitudes at $Fn=0$ in various heading angles

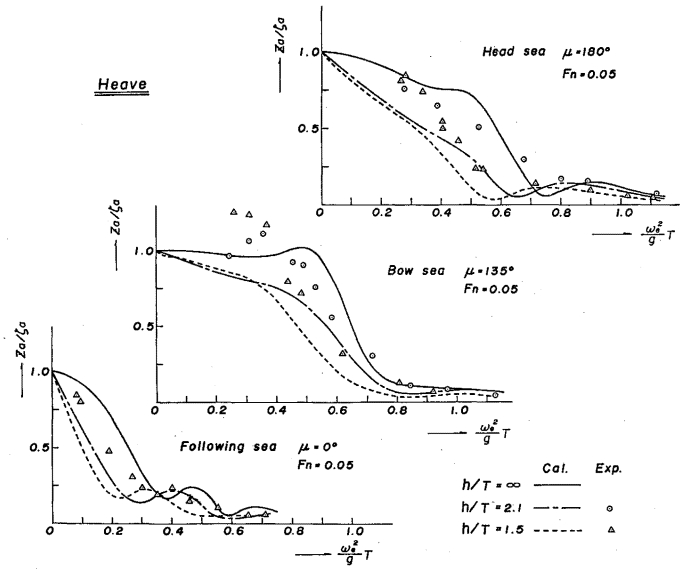


Fig. 4.2 Heaving amplitudes at $Fn=0.05$ in various heading angles

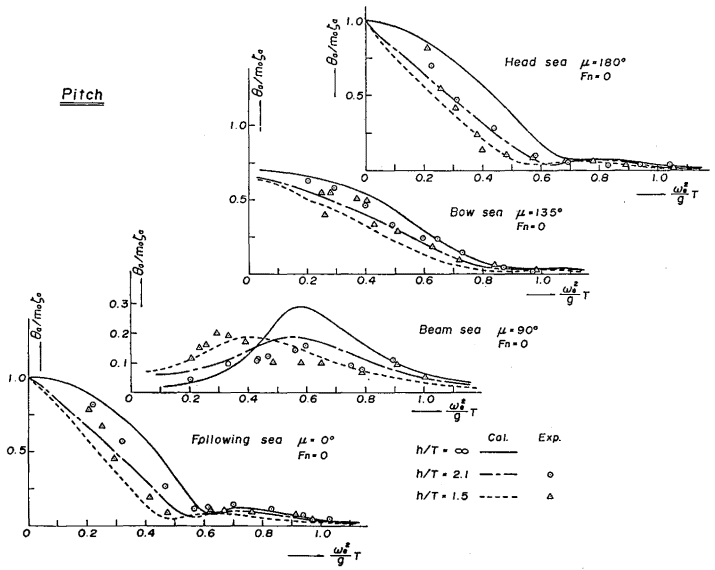


Fig. 4.3 Pitching amplitudes at $Fn=0$ in various heading angles

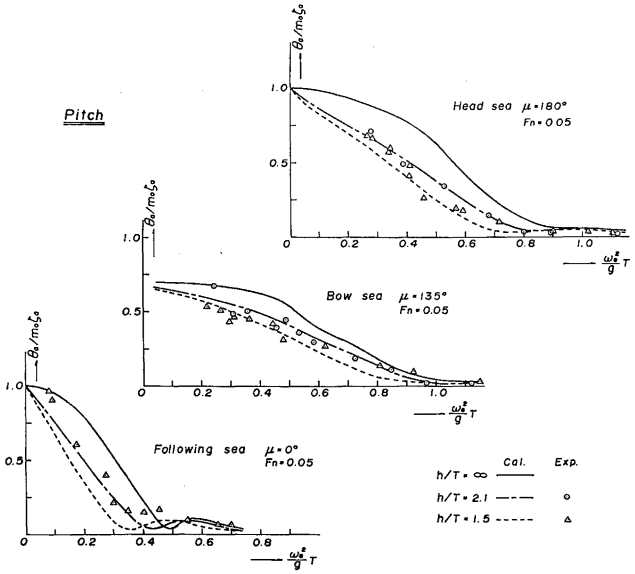


Fig. 4.4 Pitching amplitudes at $Fn=0.05$ in various heading angles

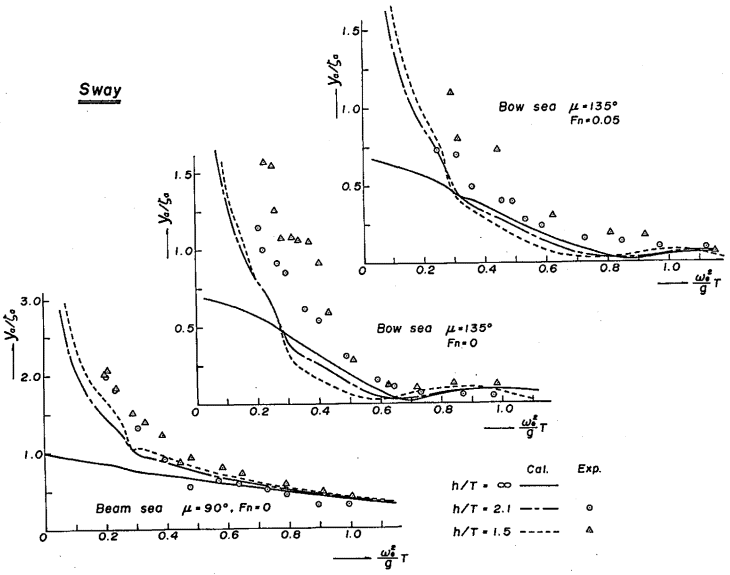


Fig. 4.5 Swaying amplitudes in various heading angles

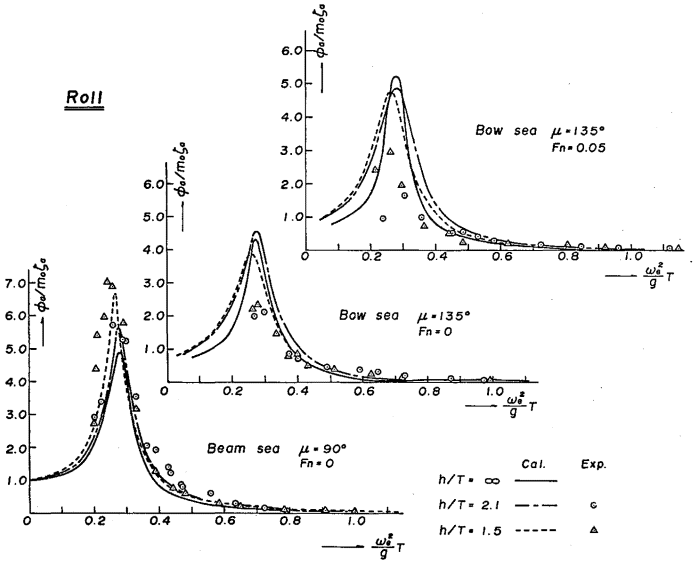


Fig. 4.6 Rolling amplitudes in various heading angles

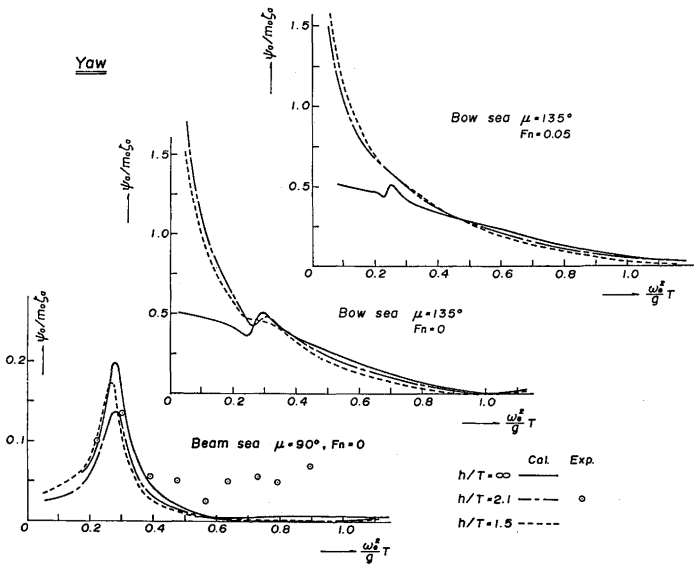


Fig. 4.7 Yawing amplitudes in various heading angles

the depths of water become more shallow shown in Fig. 2.15 and Table 2.2, the resonant peaks of rolling amplitudes do not become so large as the rate of increase of wave exciting rolling moments. These resonant peaks of rolling amplitudes do not shift to the range of low frequency so large as those of the heaving amplitudes in beam condition as the depths of water become more shallow. Because the added mass moments of inertia for rolling are much smaller than the mass moment of inertia of ship body shown in Fig. 2.14.

On the other hand, in bow condition theoretical calculations of rolling amplitudes are in fair good agreement with the experimental result except for those at resonant frequencies. Since it was very difficult to keep precisely the heading angle of ship in bow sea condition near resonant frequencies of rolling motions in this experiment, there are a few scattering points in experimental results.

(v) Yawing amplitude

Fig. 4.7 shows the yawing amplitudes in beam sea and bow sea conditions. Since the rate gyro meter was shiped water in our experiment, we could not measure the yawing amplitudes. Therefore we show the numerical results of yawing amplitudes and only the experimental results which could be measured at the water depth of 2.1 times of draft in beam sea condition. In beam sea condition the yawing amplitudes are very small but have a resonant peak due to the coupling motion of rolling near the natural period of rolling in each depth of water. The experimental results of yawing are

larger than the numerical results in high frequencies but are in good agreement with the numerical results near resonant peak due to the coupling motion of rolling.

In bow sea condition the yawing amplitudes increase rapidly in the range of low frequency ($\frac{\omega_e^2}{g}T \leqq 0.2$) and conversely decrease in other range ($\frac{\omega_e^2}{g}T \geqq 0.3$) as the depth of water become more shallow. Since yawing motion affect strongly the tension forces of mooring lines of ships moored in shallow water, it is necessary to take care of mooring ships in shallow water.

From the above discussions in (i), (ii), (iii), (iv) and (v) it is seen that theoretical values and experimental values of ship motions without a forward speed in beam sea condition agree more than those in other conditions. Because the wave exciting forces and moments on ship model in beam sea condition are evaluated precisely by using the so-called "Haskind-Newman-Bessho Relation[12]", in which a wave exciting force and moment are expressed by wave amplitude generated by ship oscillating and phase lag between ship displacement and propagating wave, while the wave exciting forces and moment on ship body in other conditions are approximately estimated by using orbital velocity and acceleration of fluid particles at the mean draft of the ship model.

## 5. Conclusion

The main conclusions obtained from the results of this study may be summarized as follows.

(1) Amplitudes of ship motions in shallow water can be estimated almost by new strip theory.

(2) The accuracies of agreements among the theoretical values and the experimental ones of ship motions in head sea, bow sea and following sea condition are not so good as those in beam sea condition in low frequencies. It seems that these are caused by the three dimensional effects of wave exciting forces and moments on a ship body.

(3) Amplitudes of swaying and yawing in beam sea and bow sea condition become larger than wave amplitudes in low frequencies as the depths of water become more shallow. Since amplitudes of swaying and yawing affect strongly the tensions of mooring lines of ship moored in shallow water, it is necessary to take care of mooring ships in shallow water.

(4) Since damping moment coefficient for rolling is affected strongly by effects of water bottom, it is necessary to study the method of estimating precisely the damping coefficient for rolling hereafter.

**Acknowledgement**

The author is grateful to Professor S. Inoue and Associate professor K. Kijima of Kyushu University who offerred willingly their experimental shallow water tank and valuable measuring meters in this experiments and to Professor F. Tasai and Associate professor M. Ohkusu for their useful suggestion and valuable discussions in this work. He also wish to express his thanks to the Engineer M. Inada, the Research student M. Egashira (at that time), Miss. M. Hojo and Miss. H. Yokobayashi for their cooperations in experiments.

The calculations of hydrodynamic forces and ones of amplitudes of ship motions were performed by means of the FACOM 230-75 of the Computer Center of Kyushu University and the FACOM 230-48 of the Computer Room of Research Institute for Applied Mechanics in Kyushu University.

It is written in addition that this study was based on the grand in aid of Ship Research 154 Meeting.

**References**

1) Kim, C. H. : The Influence of Water Depth on the Heaving and Pitching of a Ship Moving in Longitudinal Regular Head Waves, Chalmers Univ. of Tech., Dep. of Naval Architecture and Marine Eng., Division of Ship Hydrodynamics Rep. No. 44, Jun., 1968.
2) Kim, C. H. : The Influence of Water Depth on the Midship Bending Moments of a Ship Moving in Longitudinal Regular Head Waves, Chalmers Univ. of Tech., Dep. of Naval Architecture and Marine Eng., Division of Ship Hydrodynamics Rep. No. 45, Sep., 1968.
3) Hooft, J. P. : The Behaviour of a Ship in Head Waves at Restricted Water Depths, Netherlands Ship Research Center TNO, Rep. No. 188S, 1974.
4) Tuck, E. O. : Ship Motions in Shallow Water, J. of Ship Research, Vol. 14, 1970.
5) Beck, R. F. and Tuck, E. O. : Computation of Shallow Water Ship Motions, 9th Symposium on Naval Hydrodynamics, Paris, Aug., 1972.
6) Oortmessen, G. V. : The motions of ship in shallow water, S. N. A. M. E., 1975.
7) Sluijs, M. F. and Gie, T. S. : The Effect of Water Depth on Ship Motions, 14th International Towing Tank Conference, Rep. of Seakeeping Committee, Appendix 7, 1975.
8) Takaki, MI. : On the Ship Motions in Shallow Water (Part 1), Transactions of the West-Japan Society of Naval Architects, No. 50, 1975.
9) Takaki, MI. : On the Ship Motions in Shallow Water (Part 2)—Two Dimensional Hydrodynamic Coefficients for Swaying and Rolling Cylinder in Shallow Water— Transactions of the West-Japan Society of Naval Architects, No. 52, 1976.
10) Tasai, F. and Takagi, M. : Theories of response of ship motions and calculating method in regular waves, 1st Symposium of Seakeeping Quality in the Society of Naval Architects of Japan, 1969.
11) Tasai, F. : On the Sway, Yaw and Roll Motions of a Ship in Short Crested Waves, Transactions of the West-Japan Society of Naval Architects, No. 42, 1971.
12) Bessho, M. : On the Theory of Rolling Motion of Ships among Waves, Rep. of Scientific Research of Defence Academy, Vol. 3, No. 1, 1965.

13) Takaki, MI. and Tasai, F.: On the Hydrodynamic Derivative Coefficients of the Equations for Lateral Motions of Ships, Transactions of the West-Japan Society of Naval Architects, No. 46, 1973.

(Received December 7, 1977)